Measurement report: Variations in surface SO_2 and NO_x mixing ratios from 2004 to 2016 at a background site in the North China Plain

Xueli Liu[1], Liang Ran[2], Weili Lin[1*], Xiaobin Xu[3], Zhiqiang Ma[4], Fan Dong[4], Di He[4], Liyan Zhou[4], Qingfeng Shi[4], and Yao Wang[4]

[1] Key Laboratory of Ecology and Environment in Minority Areas (Minzu University of China), National Ethnic Affairs Commission, Beijing 100081, China

[2] Key Laboratory of Middle Atmosphere and Global Environment Observation, Institute of Atmospheric Physics, Chinese Academy of Sciences, Beijing, 100089, China

[3] Chinese Academy of Meteorological Sciences, Beijing, 100081, China

[4] Beijing Shangdianzi Regional Atmosphere Watch Station, Beijing, 101507, China

Correspondence to: Weili Lin (linwl@muc.edu.cn)

Abstract. Strict air pollution control strategies have been implemented in recent decades in the North China Plain (NCP), previously one of the most polluted regions in the world, and have resulted in considerable changes in emissions of air pollutants. However, little is so far known about the long-term trends of the regional background level of NO_x and SO_2, along with the increase and decrease processes of regional emissions. In this study, the seasonal and diurnal variations of NO_x and SO_2 as well as their long-term trends at a regional background station in the NCP were characterized from 2004 to 2016. On average, SO_2 and NO_x mixing ratios were 5.7 ± 8.4 ppb and 14.2 ± 12.4 ppb, respectively. The seasonal variations in SO_2 and NO_x mixing ratios showed a similar pattern with a peak in winter and a valley in summer. However, the diurnal variations in SO_2 and NO_x mixing ratios greatly differed for all seasons, indicating different sources for SO_2 and NO_x and meteorological effects on their concentrations. Overall, the annual mean SO_2 exhibited a significant decreasing trend of –6.1 % yr^{-1} (R = –0.84, P < 0.01) from 2004 to 2016, which is very close to –6.3 % yr^{-1} of the annual SO_2 emission in Beijing, and a greater decreasing trend of –7.4 % yr^{-1} (R = –0.95, P < 0.01) from 2008 to 2016. The annual mean of NO_x showed a fluctuating rise of +3.4 % yr^{-1} (R = 0.38, P = 0.40) from 2005 to 2010, reaching the peak value (16.9 ppb) in 2010, and then exhibited an extremely significant fluctuating downward trend of –4.5 % yr^{-1} (R = 0.95, P < 0.01) from 2010 to 2016. After 2010, the annual mean NO_x mixing ratios correlated significantly (R = 0.94, P < 0.01) with the annual NO_x emission in North China. The decreasing rate (–4.8 % yr^{-1}, R = –0.92, P < 0.01) of the annual mean NO_x mixing ratios from 2011 to 2016 at the Shangdianzi (SDZ) regional atmospheric background station are lower than the one (–8.8 % yr^{-1}, R = –0.94, P < 0.01) for the annual NO_x emission in the NCP and (–9.0 % yr^{-1}, R = –0.96,

$P < 0.01$) in Beijing. It indicated that surface NO_x mixing ratios at SDZ had weaker influence than SO_2 by the emission reduction in Beijing and its surrounding areas in the NCP. The increase in the amount of motor vehicles led to an increase in traffic emissions for NO_x. This study supported conclusions from previous studies that the measures taken for controlling NO_x and SO_2 in the NCP in the past decades were generally successful. However, NO_x emission control should be strengthened in the future.

1 Introduction

Acid gases sulfur dioxide (SO_2) and nitrogen oxides (NO_x) are closely related to climate, ecology, environment and human health. They are important gaseous pollutants in China (Xu et al., 2009) and also recommended by the Global Atmosphere Watch (GAW) of the World Meteorological Organization (WMO) for priority observation (WMO, 2001). They can also be transformed into nitrate and sulfate aerosols, which play an important role in the formation of aerosol pollution and acid rain (Yang et al., 2011; Cheng et al., 2013; Luo et al., 2016; Chen et al., 2017a). Sulfate and nitrate constitute more than 1/3 of $PM_{2.5}$ mass concentration and can cause serious respiratory diseases (Yang et al., 2010; Yang et al., 2011; Gao et al., 2012; Zhao et al., 2013; Liu et al., 2014a).

With the economic development, population growth and rapid urbanization, air pollution in China exhibited the characteristics of regional pollution centering urban areas in recent years (Shao et al., 2006; Xu et al., 2008). Many studies thereby focused on regional pollution (Qi et al., 2012; Li et al., 2015), instead of local and suburban pollution as previously did (Liu et al., 2008; Lin et al., 2009a). Local/suburban pollution is closely associated air pollutants emitted locally and limited on a smaller scale such as a town, a city or an urban area. Regional pollution occurs over the whole region and is usually associated with large-scale emissions and significantly influenced by transport and accompanying processes, such as chemical reactions, deposition, etc. In China, city clusters have been formed for decades, air pollution often shows regional characteristics. Especially, the North China Plain (NCP) region, a heavily industrialized and densely populated area with considerable agricultural activities, is one of the most polluted regions of the world. The strong emissions of SO_2 and NO_x in the NCP showed the typical regional characteristics (Wu et al., 2010; Lin et al., 2012; Liu et al., 2014b), i.e., similar changes in seasonal and diurnal patterns of NO_x and SO_2 had been observed at different types of sites in this region in previous studies. Previous studies have combined observations at the background site and the urban site for comparisons (Liu et al., 2014b), or selected short-term observations (1–2 years or 1–2 seasons) for the comparative study before and after major activities, in order to quantitatively evaluate the effect of implementing control measures during the event (Cheng et

al., 2015; Li et al., 2019; Lin et al., 2011a; Lin et al., 2012; Wei et al., 2016; Wu et al., 2010; Zhong et al., 2020). Most of the long-term studies (more than 10 years) evaluated the temporal and spatial variations of SO_2 and NO_x based on satellite measurements of the vertical column density (Zhang et al., 2007; Cai et al., 2018; Shikwambana et al., 2020). However, there were few studies on the long-term trend of SO_2 and NO_x based on ground-level observations (Bai et al., 2015), especially in the background area of the NCP and with a time span of more than 10 years.

In this study, we analyzed the long-term variations in surface SO_2 and NO_x mixing ratios observed at a regional WMO GAW station in the NCP, and discussed their influencing factors and their responses to pollution control measures, so as to provide scientific basis for designing further strategies for controlling SO_2 and NO_x on a regional scale.

2 Data and methods

Surface SO_2 and NO_x mixing ratios were measured at the Shangdianzi (SDZ) regional atmospheric background station (117°07′ E, 40°39′ N, 293.3 m a.s.l.). SDZ is located in Shangdianzi Village in Miyun District of Beijing, China. It is about 110 km northeast of urban Beijing. The measurements of air pollutants at this site could represent the background conditions in the NCP (Lin et al., 2008; Meng et al., 2009a).

SDZ is situated on the north hill side of a northeast-to-southwest valley, with farmlands in the south. Corn and wheat were the main crops, but were recently replaced by fruit trees. It lies in a warm temperate and semi-humid climate zone, with short spring and autumn but long winter and summer. The monthly averages of meteorological parameters such as temperature (T), pressure (P), precipitation (PRCP), relative humidity (RH), wind speed (WS) and wind direction are shown in Fig. 1. Precipitation occurs mainly in summer. The prevailing wind directions were from NE–ENE and WSW–SW. Stronger wind speeds appear in spring and weaker in summer.

In-situ measurements of SO_2 and NO_x mixing ratios were made using a pulsed fluorescence SO_2 analyzer (Model 43C-TL, Thermo Fisher Scientific, MA, USA) and a chemiluminescence NO_x analyzer (Model 42C-TL, Thermo Fisher Scientific, MA, USA), respectively. The detection limits of the Model 43C-TL SO_2 analyzer and the Model 42C-TL NO_x analyzer are 0.05 ppb (300 second averaging time) and 0.05 ppb (120 second averaging time), respectively. In Model 42C-TL NO_x analyzer, NO_2 is converted to NO by a molybdenum NO_2-to-NO converter heated to about 325°C. The conversion efficiency was checked annually using gas phase titration of an NO standard with O_3. The converter was replaced if the conversion efficiency was found lower than 96%. The drawback in this

NO_2 converter was known to suffer from the interference of other NO_y compounds such as PAN and HNO_3 (Steinbacher et al., 2007; Jung et al., 2017), which was also discussed in Yin et al. (2022). As it is not possible in our case to remove the interference, the reported NO_2 and NO_x levels should be treated as upper limits. In order to obtain long-term trends of atmospheric components at a regional atmospheric background station, the observations are required to be accurate, reliable, and comparable. Therefore, strict and effective quality control measures were implemented during the observation (Lin et al., 2019). Daily zero and span checks were routinely and automatically carried out. Multi-point calibrations were done monthly. The standard gases used at the site were compared against NIST-traceable standard gases to ensure the data comparability (Lin et al., 2009b). During the period from January 2005 to May 2017, the percentages of effective hourly mean data of SO_2 and NO_x are 97.1 % and 96.7 %, respectively. The wind speed (WS), wind direction (WD), air temperature (T), precipitation (PRCP), relative humidity (RH), and atmospheric pressure (P) during the same period are from the routine meteorological observations. We used a hybrid single-particle Lagrangian integrated trajectory model (Hysplit4.9) from National Oceanic and Atmospheric Administration, USA, with the NCEP–NCAR reanalysis meteorological data set (https://ready.arl.noaa.gov/archives.php) to calculate the atmospheric mixed layer heights.

3 Results

3.1 Observational levels

The time series and statistic results of hourly mean SO_2 and NO_x mixing ratios during the observational period at SDZ are showed in Fig. 2 and Table 1, respectively. The hourly mean SO_2 mixing ratios ranged from 0.01 to 100.34 ppb, with 193 hours (0.18 %) exceeded the limit of 57 ppb set in China National Ambient Air Quality Standard (GB3095–2012, Grade I). The hourly mean NO_2 mixing ratios ranged from 0.01 to 124.4 ppb, with 5 hours exceeding the limit of 106 ppb (GB3095–2012, Grade I). The SO_2 mixing ratios exhibited an extremely significant downward trend (–0.37 ppb yr^{-1}, R = –0.20, $P < 0.01$) during the measurement period and a higher downward trend (–1.10 ppb yr^{-1}, R = –0.22, $P < 0.01$) from 2013 to 2017. The NO_x mixing ratios exhibited a much smaller but significant downward trend (–0.03 ppb yr^{-1}, R = –0.01, $P < 0.05$). Details in the trends and the influencing factors will be discussed in Sect. 3.4.

As shown in Table 1, the average values ± 1σ (standard deviation) of SO_2, NO, NO_2, and NO_x concentrations are 5.7 ± 8.4 ppb, 1.1 ± 2.6 ppb, 13.1 ± 10.9 ppb, and 14.2 ± 12.4 ppb, respectively. The results were close to the annual average concentrations of SO_2 (5.9 ± 10.0 ppb), NO (0.8 ± 2.0 ppb), NO_2 (13.8 ± 13.1 ppb), and NO_x (14.5 ± 14.0

ppb) at SDZ in 2004 reported by Meng et al. (2009a). Compared with other background stations in China (Table 2), the SO_2 and NO_x mixing ratios at SDZ are both at a relatively high level.

3.2 Monthly variations

Surface SO_2 and NO_x mixing ratios at SDZ showed a similar seasonal pattern with high values in winter and low values in summer (Fig. 3). The highest SO_2 level appeared in winter (9.46 ppb) with the maximum monthly mean in February (10.57 ppb), followed by that in spring (7.28 ppb) and autumn (5.01 ppb), and the lowest in summer (2.06 ppb) with the minimum in July (1.45 ppb). The concentration of NO_x was higher in winter (18.12 ppb) and autumn (16.51 ppb), lower in spring (12.95 ppb) and summer (9.24 ppb). The maximum monthly mean NO_x appeared in November (21.70 ppb) and the minimum one in August (8.69 ppb). The seasonal patterns of SO_2 and NO_x at SDZ were similar to those in urban and rural areas in North China (Meng et al., 2009b; Lin et al., 2012; Song et al., 2016; Tang et al., 2016; Chen, 2017b; Zhao et al., 2020), which were characterized by high levels in the heating period and low levels in summer.

The heating period in North China was from November to March. Coal burning was used to be the major source for heating in the NCP, but it has been gradually substituted by natural gas since 2013 in urban areas. In the rural areas, however, there was still burning of coal and wood for heating. The emissions of SO_2 and NO_x in the heating period were higher than those in the non-heating periods. Compared with the non-heating period, lower temperature, drier air, weaker solar radiation, less precipitation, and lower mixing depth heights were found in the heating period, resulting in lower atmospheric chemical reaction rate of SO_2 and NO_x, smaller removal effect of precipitation, weaker vertical diffusion, longer atmospheric lifetime, and thus higher concentrations.

3.3 Diurnal variations

The average diurnal variations in SO_2 and NO_x mixing ratios at SDZ in different seasons are shown in Fig. 4. The SO_2 mixing ratios peaked at 11:00 in spring and summer, 14:00 in fall, and 21:00 in winter. The NO_x mixing ratios peaked at 1:00 in winter, 2:00 in spring, fall and summer. In addition, the valley of SO_2 diurnal cycle appeared at 5:00 in spring and summer, 6:00 in fall and winter, whereas for NO_x it was at 12:00 in spring, 13:00 in summer, 13:00 in fall, and 12:00 in winter, respectively. The diurnal behaviors of NO_x and SO_2 mixing ratios are different. Generally, the average daily amplitudes of SO_2 are 3.0 ppb in spring, 2.0 ppb in summer, 4.4 ppb in fall, and 3.7 ppb in winter, respectively, while the average daily amplitudes of NO_x are 6.8 ppb in spring, 6.3 ppb in summer, 10.6 ppb in fall and 10.5 ppb in winter, respectively.

3.4 Long-term trends of SO_2 and NO_x mixing ratios

Figure 5a shows the annual mean SO_2 mixing ratios from 2004 to 2016 at SDZ site, as well as the annual SO_2 emissions in North China (including Beijing, Tianjin, Hebei, Shanxi and Inner Mongolia). The annual mean SO_2 mixing ratio in 2004 was from Meng et al. (2009a). The SO_2 emission peaked in 2006 and then decreased with years. Meanwhile, the annual mean SO_2 mixing ratio reached a high level around 7.6 ppb during 2006-2008, and then began to decline thereafter. A rebound in SO_2 emission occurred in 2011, while a lagged rise of SO_2 mixing ratio occurred in 2012. Overall, the annual mean SO_2 exhibited a significant decreasing trend of –0.36 ppb yr^{-1} (–6.1 % yr^{-1}, R = –0.84, $P < 0.01$) from 2004 to 2016 and a greater decreasing trend of –0.56 ppb yr^{-1} (–7.4 % yr^{-1}, R = –0.95, $P < 0.01$) from 2008 to 2016.

Figure 5b shows the long-term variations in the annual 5th and 95th percentile values of the hourly mean SO_2 in different years. The 95th percentile indicated the influence of polluted air masses, while the 5th percentile indicated the influence of clean air masses. Similar to the trends of annual mean SO_2 mixing ratios, the 95th percentile of SO_2 reached its peak (30.87 ppb) in 2007, and a little decrease in 2008 (29.19 ppb). After 2008, it began to decline. Compared with the SO_2 level in 2008, there was a great decrease (–19.8 %) in 2009, but from 2009 to 2012 there was no significant decline in annual mean of SO_2. The most significant downward trend of the 95th percentile of SO_2 was found from 2012 to 2016 with a rate of –3.98 ppb yr^{-1} (–16.3 % yr^{-1}, R = –0.99, $P < 0.01$). However, the 5th percentile of SO_2 mixing ratios did not change significantly of –0.05 ppb yr^{-1} (–2.6 % yr^{-1}, R = –0.15, P = 0.6) from 2005 to 2016.

The annual mean of NO_x shows an increasing trend of +0.37 ppb yr^{-1} (+3.4 % yr^{-1}, R = 0.38, P = 0.40) from 2005 to 2010 with strong fluctuations (Fig. 5c,d). The annual NO_x mean reached the peak value (16.93 ppb) in 2010, and exhibited a significant downward trend of –0.77 ppb yr^{-1} (–4.5 % yr^{-1}, R = 0.95, $P < 0.01$) from 2010 to 2016 (Fig. 5c). The 95th percentile of the hourly mean of NO_x firstly increased during 2005-2012 with +0.02 ppb yr^{-1} (+0.1 % yr^{-1}, R = 0.73, $P < 0.05$) and then decreased during 2012–2016 with –0.03 ppb yr^{-1} (–4.7 % yr^{-1}, R = 0.95, $P < 0.05$). Similar to SO_2, the annual 5th percentile of NO_x mixing ratios did not change significantly (–1.7 % yr^{-1}, R = –0.18, P = 0.58) from 2005–2016 (Fig. 5d).

We regrouped NO_x and SO_2 data into 4 subsets according to the heating period (November–March), spring (April–May), summer (June–August), and autumn (September–October). The long-term trends of the four subsets are shown in Fig. 6. The SO_2 mixing ratios showed significant downward trends of –0.96 ppb yr^{-1} (–8.0 % yr^{-1}, R = –0.99, $P < 0.01$) in the heating period, –0.39 ppb yr^{-1} (–5.2 % yr^{-1}, R = –0.84, $P < 0.01$) in spring, –0.24 ppb yr^{-1}

(–4.3 % yr^{-1}, R = –0.92, P < 0.01) in autumn, and –0.18 ppb yr^{-1} (–7.7 % yr^{-1}, R = –0.87, P < 0.01) in summer. The large reduction in the SO_2 level in the heating period was largely related to burning natural gas instead of coal for domestic heating (Qiu et al., 2017; Li et al., 2020).

Except for autumn, the trends of the annual mean NO_x mixing ratios in other seasons showed a similar pattern that NO_x mixing ratio rose firstly and then declined significantly. The annual mean of NO_x in autumn showed a downward but statistically insignificant trend of –0.08 ppb yr^{-1} (–0.6 % yr^{-1}, R = –0.28, P = 0.38) from 2005 to 2016. In other seasons, the peaks of NO_x appeared in different years. The NO_x mixing ratios showed significant downward trends of –1.16 ppb yr^{-1} (–5.4 % yr^{-1}, R = –0.84, P < 0.05) in the heating period during 2012–2016, –1.07 ppb yr^{-1} (–7.6 % yr^{-1}, R = –0.96, P < 0.01) in spring during 2012–2017, and –0.67 ppb yr^{-1} (–4.5 % yr^{-1}, R = –0.87, P = 0.01) in summer during 2011–2016.

4 Discussion

4.1 The influence of emission control on long-term trends of NO_x and SO_2

The annual mean and the 95th percentile of SO_2 mixing ratios at SDZ from 2004 to 2016 were significantly correlated with the annual SO_2 emissions in North China with correlation coefficients of 0.85 (P < 0.01) and 0.88 (P < 0.01), respectively. The decreasing rates of annual mean and 95th percentile of SO_2 mixing ratios from 2004 to 2016 at SDZ were –6.1 % yr^{-1} and –6.2 % yr^{-1}, respectively, which were higher than the trend (–3.1 % yr^{-1}) of the annual SO_2 emission in the NCP, but very close to the trend (–6.3 % yr^{-1}) of the annual SO_2 emission in Beijing. This indicated that surface SO_2 mixing ratios at SDZ were more influenced by the emission in Beijing than other provinces in the NCP.

There seemed a lag between the variation of SO_2 mixing ratios and the emissions (Fig. 5a,b; Fig. S1a,b) and surface SO_2 mixing ratio in 2012 was evidently inconsistent with the emission trend, which indicated the complexity of the effect of reducing SO_2 emission on SO_2 mixing ratios. The effectiveness and timing of pollution control policies, as well as the change of meteorology year by year, would cause their asynchronous trends. China has implemented a series of stringent clean air actions from 2013 to 2017, and the "*Beijing 2013-2017 Clean Air Action Plan*" was the most comprehensive and systematic pollution control program in Beijing (UN Environment, 2019). Before 2013, there would be some emissions being not counted for some reasons by local government, as the change in the 95% percentile of SO_2 mixing ratios did not show a similar decreasing trend of the mean SO_2 mixing ratios from 2009 to 2011. Another reason would be the change in SO_2 mixing ratios at the SDZ regional

background site was not as obvious as the change in Beijing urban and other polluted areas as Lin et al. (2012) had stated. Changes in meteorology would also lead to a decoupling of emissions and measured SO_2 and NO_2 values, but it cannot be quantified how much the changes contributed to this time shift.

Taking 2008 as the base year, a stronger decreasing trend of –7.4 % yr^{-1} (R = –0.95, P < 0.01) from 2008 to 2016 for the annual mean SO_2 mixing ratio can be found, as well as a significant decreasing rate of (–4.5 % yr^{-1}, R = –0.81, P < 0.01) for the annual 5 % percentile of SO_2 mixing ratios. More strict emission control measures had been implemented for the 2008 Beijing Olympic Games, where the SO_2 pollution control had long-term effects and benefits as Lin et al. (2012) had pointed out. Surface SO_2 mixing ratios in Beijing in the first half year of 2008 before the Olympic game, held in August and September, showed higher values than that in the rest of the year (Lin et al., 2012). We believe the higher emission before the Olympics was due to more activities in preparing the Olympic game. Although more reduction in SO_2 was seen in the post-Olympics period, the SO_2 mixing ratio showed a higher annual mean in 2008 than in 2009. Theoretically, the worldwide economic crisis in 2009 might cause a lower level of SO_2 but considering the economic stimulation measures implemented by the government, we do not think the economic crisis played a significant role. Moreover, the higher NO_x emission in 2009 than in 2008 supports our view. The improvement of energy structure has been speeded up in Beijing from 2009, which might be a more important factor. An assessment by the United Nations Environment Programme reported that the significant decline in SO_2 mixing ratios and emissions from 1997–2017 was largely due to the SO_2 control measures in Beijing and the surrounding areas, especially the transformation of coal-fired boilers, energy structure adjustments and the end treatment of SO_2 tail gas (UN Environment, 2019). The SO_2 observation at SDZ background site confirmed the effect of SO_2 reduction.

Before 2011, the annual mean NO_x showed an increasing trend with fluctuation year by year. There is a steep increase in NO_x in 2010, as well as that in 2006. It is worth noting that the motor vehicles in Beijing in 2010 had increased significantly from the previous year (see Figure S2), since the policy of purchase restriction in motor vehicle was implemented in 2011. In addition, NO_x emissions from power plants and industrial sources were not strictly controlled before 2011. Therefore, more NO_x would be emitted in years with prosperous economy. According the analysis by Krotkov et al. (2016) and Duncan et al. (2016), NO_2 pollution over Northeast China has reached its peak in 2011, and there have large decreases over Beijing, Shanghai, and the Pearl River Delta, which were likely associated with local emission control efforts. Beijing has adopted the policy of "new car purchase restriction" lottery number purchase since January 1, 2011 and has implemented the plan for further promoting the elimination and renewal of old cars since August 1, 2011. New glass emission standard for air pollutants from the

flat glass industry (GB 26453-2011) was also implemented in this year. After 2010, the annual mean and 95th percentile of NO_x mixing ratios correlated significantly (R = 0.94, P < 0.01 and R = 0.82, P < 0.05, respectively) with the annual NO_x emission in North China, but the NO_x mixing ratios exhibited more fluctuations than NO_x emissions (Fig. 5c, 5d). As shown in Fig. S1c and S1d, the annual mean NO_x mixing ratios were also significantly correlated with the NO_x emission in Beijing (R = 0.93, P < 0.01) from 2010 to 2016 (Fig. S1c). However, the 95th percentile of NO_x did not show a significant correlation (R = 0.80, P = 0.06) (Fig. S1d), indicating that high values of NO_x at SDZ may be much more affected by NO_x emissions from other North China regions than Beijing. The decreasing rates of –4.8 % yr^{-1} (R = –0.92, P < 0.01) for the annual mean and –4.5 % yr^{-1} (R = –0.82, P < 0.05) for the 95th percentile NO_x mixing ratios from 2011 to 2016 at SDZ were lower than the one (–8.8 % yr^{-1}, R = –0.94, P < 0.01) for the annual NO_x emission in the NCP and (–9.0 % yr^{-1}, R = –0.96, P < 0.01) in Beijing. Unlike the annual mean or 95th percentile values, the 5th percentile of NO_x mixing ratios from 2011 to 2016 did not exhibit a significant trend (–5.0 % yr^{-1}, R = –0.54, P = 0.27) at SDZ.

It indicated that surface NO_x mixing ratios at SDZ was relatively weakly influenced by the emission reduction in Beijing and its surrounding areas in the NCP compared with the condition of SO_2, probably because there were more emission sources for NO_x than for SO_2. For example, although the coal-burning source pollution control measures adopted in the *the Clean Air Action* have helped to reduce NO_x emissions, the increase in the amount of motor vehicles led to an increase in NO_x emission from the traffic (Fontes et al., 2018; Sun et al., 2018; Zhang et al., 2019; Zhang et al., 2020). In addition, the change of atmospheric transport conditions and the expansion of urban scale may lead to the downward trend of NO_x, but not as obvious as that of SO_2 at SDZ (Lin et al., 2012). Fortunately, NO_x pollution control measures on coal-burning source and vehicle pollution had also begun to achieve more significant outcome since 2011 (Krotkov et al., 2016; UN Environment, 2019). Especially, vehicle pollution control was strengthened through the improvement of oil quality and promotion of new energy vehicles. As a result, Beijing's motor vehicle growth rate decreased from 19.7 % in 2010 to 3.6 % in 2011 and the number of new energy vehicles had an increase of 431 % from 2013 to 2016 (Figure S2).

4.2 Variations in NO_x and SO_2 mixing ratios in different periods

We regrouped the NO_x and SO_2 data into 4 subsets in 4 different time stages (Stage I: 2005–2008, Stage II: 2009–2012, Stage III: 2013–2014, and Stage IV: 2015–2017). Key pollution control measures had been implemented in different stages, e.g., emission controls for the 2008 Beijing Olympic Games, *the State Council Air Pollution Prevention and Control Action Plan (Action Plan 2013–2017)* and *Beijing 2013–2017 Clean Air Action*

Plan. Details of the pollution prevention plans and its implementation can be found in UN Environment (2019) and in Zheng et al. (2018), in which, control process and specific measures for coal combustion and motor vehicles in Beijing from 1998 to 2017, and China's clean air policies implemented during 2010–2017 had been reviewed. Since 2015, the government of Beijing–Tianjin–Hebei region has promoted the application of electric energy substitution using electric energy instead of traditional fossil energy (Wang et al., 2020).

The average diurnal variations in SO_2 and NO_x at SDZ in four stages are shown in Fig. 7 and Fig. S3. The SO_2 levels and their amplitudes of the average diurnal variation continued to decrease as the stage time went by. The differences in SO_2 among the 4 different periods are significant ($P<0.001$) from the One-Way ANOVA test, and the differences between the two groups are also significant ($P<0.01$) from t-test. The diurnal amplitude of SO_2 was 4.16 ppb in Stage I and 0.94 ppb in Stage IV. The peak time of SO_2 in Stage IV appeared at 11:00 instead of the former 16:00. The peak value decreased significantly, from 9.38 ppb in Stage I to 3.19 ppb in Stage IV, with a factor of –66.0 %. This phenomenon indicated that the control measures implemented in the period 2013–2017 have not only had notable effects in reducing emissions from power plants, but also had significant achievement in the emission control of non-electric industries such as industrial boilers and kilns (Zhang et al., 2019), which made the emission intensity of SO_2 pollutants from elevated sources weaker than that in the Stage I.

Different from SO_2, the average diurnal of NO_x mixing ratios did not show a gradual decrease over time and with values of Stage II > Stage III > Stage I > Stage IV. For NO_x, the differences among the 4 different periods are significant ($P=0.01$) from the One-Way ANOVA test, but the differences between the two groups are only significant ($P<0.01$) between Y2009-2012 and Y2015-2017 from t-test. In addition, the diurnal variations and the diurnal amplitude of NO_x did not change much with the daily amplitudes being about 8.52 ppb. The peak and valley appeared respectively at about 2:00 and at about 13:00 in 4 stages. The increase of NO_x and the decreasing of SO_2 in Stage II tells the fact of much more effective of pollution control measures on SO_2 rather than NO_x implemented in Beijing and other places. China intensified its acid rain control in the beginning of this century by much more strict control of SO_2 emissions from coal-fired power plants. However, the control of NO_x emissions remained weak until the introduction of the new Emission Standard of Air Pollutants for Thermal Power Plants (GB13223-2011) (Wang et al., 2019). Such major difference in SO_2 and NO_x emission control caused an earlier peak for SO_2 (around 2006) and a later peak for NO_x (around 2011-2012) (Li et al., 2017). The emission data for North China (Figure 5) nearly resemble the nationwide situation and the mixing ratio data at SDZ (Figure 7) are consistent with the general trends of SO_2 and NO_x emissions. At the same time, the amount of motor vehicles has been rapidly increasing, resulting in an increase in NO_x emissions from vehicle exhaust.

Figure 8 shows the rose maps of SO_2 and NO_x mixing ratios in 4 different time periods (Figure S4 and S5 are rose maps in different seasons, Table S1 is frequency distributions of wind directions in different stages). High NO_x values were in broader wind sectors except NW–NNW–N–NNE, whereas high SO_2 values were mainly in W–WSW–SW–SSW sectors. Except for the SSW sector, SO_2 mixing ratios in other wind directions showed a decreasing trend over stages. Both the severely polluted areas and the slightly polluted areas have the same characteristics of decreasing in SO_2 level over time (Table 3). Unlike the highest SO_2 mixing ratio being in Stage I (2005–2008), the highest NO_x mixing ratios was in Stage II (2009–2012). The overall levels of SO_2 and NO_x in the Stage IV reached the lowest values among the four stages. Compared with those at the stage with the highest mixing ratios of NO_x and SO_2, the reduction ranges in Stage IV are 52.2 %–76.4 % for SO_2 and 3.8 %–45.3 % for NO_x in different wind sectors. Much more reduction in SO_2 than NO_x indicates that the electric energy substitution policy in Beijing–Tianjin–Hebei region has been much more effective on SO_2 reduction than NO_x.

The SO_2/NO_x ratio, obtained from the reduced major axis regression of the daily mean SO_2 and NO_x mixing ratios, exhibited a significant change from 0.84 during 2005–2008 to 0.30 during 2015–2017. The possible reason for this phenomenon was that the control measures including the upgrading of end treatment facilities of coal-fired power plants, the conversion of coal to clean energy, and the elimination of coal-fired boilers, which were taken in the early stage of *the Clean Air Action*, had greatly reduced SO_2 emissions rather than NO_x. Another reason could be an increase in the number of motor vehicles (Figure S2) and relatively more difficulties in emission control on the mobile sources. Unlike emissions from industries, emissions from automobiles are relatively more difficult to control. The reason that supports this argument is that emissions from industrial plants could be quantitatively measured, thus control measures that require a reduction of a certain percentage in emissions could be implemented. However, the estimation of emissions from automobiles bears large uncertainties in the first place. Though there are also strict control regulations as to cars with license plates of a chosen number are not allowed to be on road on certain days, the actual reduction in emissions also depends on the usage of other cars.

In the period of 2005–2012, the construction of new power plants and the amount of motor vehicle ownership rapidly increased in the city. During this period, flue gas desulfurization devices have been widely used (Zhao et al., 2008). However, the main management measures that required power plants to deploy denitrification devices for reducing NO_x emissions, have not been implemented until 2012, resulting in the increase of nitrogen oxide emissions (Wang et al., 2010; Wang and Hao, 2012; Liu et al., 2016), and the contribution to the transport of NO_x to SDZ during this period.

306 **4.3 The different diurnal behaviors in SO_2 and NO_x mixing ratios and their source origin**

307 The seasonal variations in SO_2 and NO_x mixing ratios exhibited a similar pattern with high values in winter and low
308 values in summer, and their daily mean values had a significant correlation (R = 0.59, P < 0.01). However, the
309 diurnal variations in SO_2 and NO_x mixing ratios were greatly different from each other (Figure 9). Due to the
310 increased emissions, lower mixing depth and slower chemical conversions in winter, SO_2 values showed significant
311 diurnal behavior in winter which was different from other seasons. Except for the winter, the SO_2 mixing ratios were
312 higher during the daytime and lower during the nighttime in all seasons, while the NO_x mixing ratios showed an
313 opposite pattern. The different diurnal behaviors in SO_2 and NO_x at SDZ might indicate a different origin of SO_2 and
314 NO_x.

315 Due to the diurnal variation in the boundary layer, the mixing depth is higher during the daytime and the convective
316 mixing is strong, which is conducive to the dilution and diffusion of pollutants. The photochemical reaction during
317 the daytime is also conducive to the chemical transformation of pollutants. At night, the pollutants are easy to
318 accumulate because of lower mixing depth and no photochemical processes. Therefore, the concentration of primary
319 pollutants exhibits higher values during the nighttime and lower during the daytime in general. But the situation for
320 SO_2 at SDZ was different. The higher SO_2 mixing ratios during the daytime suggested two possible mechanisms: (1)
321 an elevated level of SO_2 aloft, which could be mixed downward to the ground due to the evolution of atmospheric
322 boundary layer, causing higher ground-level SO_2 concentrations in the daytime. (2) upwind SO_2 sources and
323 transport of plumes in the daytime.

324 Since the SDZ station is selected as WMO/GAW regional station, local anthropogenic emissions are well avoided.
325 As SDZ is located on the north side of a valley with a northeast-southwest orientation, its dominant wind directions
326 were from southwest and northeast with regular changes in diurnal wind directions (Figure S6). The southwest
327 mouth of the valley is open to the NCP, so it is easily influenced by the air masses from the south polluted areas,
328 like urban Beijing. As a result, the concentration rose maps of pollutants exhibited higher values in the southwest
329 sectors than other sectors (Lin et al., 2008; Meng et al., 2009a). If only due to the influence by advection transport,
330 the diurnal variations in SO_2 and NO_x at SDZ should be similar. However, the two show obvious differences. The
331 higher SO_2 mixing ratios during the daytime indicates an elevated level of SO_2 in a high air layer, which can be
332 exchanged to the surface under the evolution of atmospheric boundary layer, causing a higher SO_2 value in the
333 daytime. The 'unusual' phenomenon of the diurnal change in SO_2 has been noticed and explained by studies (Lin et
334 al., 2008; Chen et al., 2009; Xu et al., 2014), but it lacked direct vertical profile measurements to support this

explanation. The daytime peak of SO_2 was not only found at SDZ, but also at different sites in urban and rural areas in North China (Lin et al., 2012) and in the background area of the Yangtze River Delta (Qi et al., 2012). This may be related to the fact that SO_2 is mainly emitted from elevated sources (Lin et al., 2012; Xu et al., 2014). The daily maximum of SO_2 concentrations was caused by the downward mixing of SO_2 emitted by elevated sources in this region. As strict and effective control measures were continuously implemented, the contribution from such a source largely decreased and finally became negligible. Governed by the development of the planetary boundary layer, the diurnal variation of SO_2 concentrations would peak around noon. This may be the cause of the shift in time of the SO_2 maximum as mentioned in Section 4.2. Xu et al. (2014) have discussed the implications of this SO_2 noontime-peak phenomenon in sulphur deposition and transformation. At night, prevail north wind transported clean air to SDZ. This process should be the major cause of the decreasing SO_2 levels during nighttime, since surface SO_2 mixing ratios depend on vertical air exchange. Enhanced relative humidity during nighttime should be also a loss effect since SO_2 is a very soluble gas. In addition, dry deposition of SO_2 in a shallow nocturnal boundary layer might lower the SO_2 level as well.

It can be seen that the NO_x mixing ratios began to rise around noontime when the mixing depth was still elevating (Figure 9). Obviously, NO_x was affected by the transport of pollutants in the southern polluted area during the noontime when the WD changed into southwest wind (Figure S6). Of course, motor vehicles running on the roads and dispersing human activities can emit NO_x as well as the transport from the south. As seen in Figure 8, the NO_x rose map showed wider source origins than SO_2. However, SO_2 maintained a relatively high value instead of increasing significantly, indicating that SO_2 mixing ratios were still mainly affected by downward mixing of SO_2-richer air.

Conclusion

Measurements of surface NO_x and SO_2 mixing ratios at SDZ regional atmospheric background site in the North China Plain from the period 2005–2017, together with ancillary data, were summarized and used to study their long-term trends and influencing factors. The average values ± 1σ (standard deviation) of SO_2 and NO_x mixing ratios were 5.7 ± 8.4 ppb and 14.2 ± 12.4 ppb, respectively. The seasonal variation in SO_2 and NO_x at SDZ showed a similar pattern with high values in winter and low values in summer, but the diurnal variations in SO_2 and NO_x mixing ratio exhibited large differences in all seasons. The SO_2 mixing ratios were higher during the daytime and lower during the nighttime, while the NO_x mixing ratios showed higher values during the nighttime and lower

during the daytime. The different diurnal behaviors in SO_2 and NO_x at SDZ indicated a different origin of SO_2 and NO_x.

Overall, the annual mean SO_2 exhibited a significant decreasing trend of –0.36 ppb yr^{-1} (–6.1 % yr^{-1}, R = –0.84, P < 0.01) from 2004 to 2016 and a greater decreasing trend of –0.56 ppb yr^{-1} (–7.4 % yr^{-1}, R = –0.95, P < 0.01) from 2008 to 2016. The decreasing rates of annual mean and 95th percentile of SO_2 mixing ratios from 2004 to 2016 at SDZ are very close to the one (–6.3 % yr^{-1}) of the annual SO_2 emission in Beijing. The annual mean of NO_x showed a fluctuating rise of +0.37 ppb yr^{-1} (+3.4 % yr^{-1}, R = 0.38, P = 0.40) from 2005 to 2010, reaching the peak value (16.93 ppb) in 2010, and then exhibited an extremely significant fluctuating downward trend of –0.77 ppb yr^{-1} (–4.5 % yr^{-1}. R = 0.95, P < 0.01) from 2010 to 2016. After 2010, the annual mean and 95 % percentile of NO_x mixing ratios correlated significantly (R = 0.94, P < 0.01 and R = 0.82, P < 0.05, respectively) with the annual NO_x emission in North China. The decreasing rates of –4.8 % yr^{-1} (R = –0.92, P < 0.01) for the annual mean and –4.5 % yr^{-1} (R = –0.82, P < 0.05) for the 95th percentile NO_x mixing ratios from 2011 to 2016 at SDZ are lower than the one (–8.8 % yr^{-1}, R = –0.94, P < 0.01) for the annual NO_x emission in the NCP and (–9.0 % yr^{-1}, R = –0.96, P < 0.01) in Beijing. It indicated that surface NO_x mixing ratios at SDZ had a weaker response to the emission reduction in Beijing and its surrounding areas in NCP than SO_2. The increase in the amount of motor vehicles and the weak effectiveness of traffic restrictions have caused motor vehicle emissions on NO_x.

Data availability. The data in this study can be publicly accessed via https://doi.org/10.7910/DVN/YFVLHV (Liu et al., 2022).

Author contributions. XL wrote the paper, WL developed the idea, formulated the research goals, and edited the paper. LR, XX and ZQ edited the paper. WL, FD, DH, LZ, QS and YW carried out the measurement of NO_x and SO_2, and analysed the meteorological data.

Competing interests. The authors declare that they have no conflict of interest.

Acknowledgements. This study was funded by the National Natural Science Foundation of China (Grant No. 91744206) and the Open Fund of Shangdianzi Atmospheric Background Station (SDZ2020615).

References

Bai, J., Wu, Y., Chai, W., Wang, P., and Wang, G.: Long–term variation of trace gases and particulate matter at an atmospheric background station in North China (in Chinese), Advances in Geosciences., 5, 248-263, https://doi.org/10.12677/AG.2015.53025, 2015.

Cai, K., Zhang, Q., Li, S., Li, Y., and Ge, W.: Spatial-temporal variations in NO_2 and $PM_{2.5}$ over the Chengdu–Chongqing economic zone in China during 2005 – 2015 based on satellite remote sensing, Sensors-Basel., 18, 3950, https://doi.org/10.3390/s18113950, 2018.

Chen, L.: Measure and study on the atmospheric pollutants in three typical regional background stations of China (in Chinese), Master, Lanzhou University, 2012.

Chen, T., Chang, K., and Tsai, C.: Modeling approach for emissions reduction of primary $PM_{2.5}$ and secondary $PM_{2.5}$ precursors to achieve the air quality target, Atmos. Res., 192, 11-18, https://doi.org/10.1016/j.atmosres.2017.03.018, 2017a.

Chen, C.: Analysis of atmospheric pollutants characteristics in the typical suburban station of North China (in Chinese), Master, Nanjing University of Information Science and Technology, 2017b.

Chen, Y., Zhao, C., Qiang, Z., Deng, Z., Huang, M., and Ma, X.: Aircraft study of mountain chimney effect of Beijing, China, J. Geophys. Res-atmos., 114, D8306, https://doi.org/10.1029/2008JD010610, 2009.

Cheng, M., Pan, Y., Wang, H., Liu, Q., and Wang, Y.: On-line measurement of water-soluble composition of particulate matter in Beijing (in Chinese), Environ. Sci., 34, 2943-2949, https://doi.org10.13227/j.hjkx.2013.08.018, 2013,

Cheng, N., Chen, T., Zhang, D., Li, Y., Sun, F., Wei, Q., Liu, J., Liu, B., and Sun, R.: Air quality characteristics in Beijing during Spring Festival in 2015 (in Chinese), Environ. Sci., 36, 3150-3158, https://doi.org/10.13227/j.hjkx.2015.09.005, 2015.

Cheng, L., Ji, D., He, J., Li, L., Du, L., Cui, Y., Zhang, H., Zhou, L., Li, Z., and Zhou, Y.: Characteristics of air pollutants and greenhouse gases at a regional background station in Southwestern China, Aerosol Air Qual. Res., 19, 1007-1023, https://doi.org/10.4209/aaqr.2018.11.0397, 2019.

Fontes, T., Li, P., Barros, N., and Zhao, P.: A proposed methodology for impact assessment of air quality traffic-related measures: The case of $PM_{2.5}$ in Beijing, Environ. Pollut., 239, 818-828, https://doi.org/10.1016/j.envpol.2018.04.061, 2018.

Gao, J., Zhang, Y., Wang, S., Chai, F., and Chen, Y.: Study on the characteristics and formation of a multi-day haze in October 2011 in Beijing (in Chinese), Res. Environ. Sci., 25, 1201-1207, https://doi.org/CNKI:SUN:HJKX.0.2012-11-002, 2012.

Jung, J., Lee, J., Kim, B., and Oh, S.: Seasonal variations in the NO_2 artifact from chemiluminescence measurements with a molybdenum converter at a suburban site in Korea (downwind of the Asian continental outflow) during 2015–2016, Atmos. Environ., 165, 290-300, https://doi.org/10.1016/j.atmosenv.2017.07.010, 2017.

Krotkov, N. A., Mclinden, C. A., Li, C., Lamsal, L. N., Celarier, E. A., Marchenko, S. V., Swartz, W. H., Bucsela, E. J., Joiner, J., and Duncan, B. N.: Aura OMI observations of regional SO_2 and NO_2 pollution changes from 2005 to 2015, Atmos. Chem. Phys., 16, 4605-4629, https://doi.org/10.5194/acp-16-4605-2016, 2016.

Li, F., Tan, H., Deng, X., Deng, T., Xu, W., Ran, L., and Zhao, C.: Characteristics analysis of sulfur dioxide in Pearl River Delta from 2006 to 2010 (in Chinese), Environ. Sci., 5, 1530-1537, https://doi.org/CNKI:SUN:HJKZ.0.2015-05-003, 2015.

Li, M., Liu, H., Geng, G., Hong, C., Liu, F., Song, Y., Tong, D., Zheng, B., Cui, H., Man, H., Zhang, Q. and He, K.: Anthropogenic emission inventories in China: a review, National Science Review, 4, 834–866, https://doi.org/10.1093/nsr/nwx150, 2017.

Li, Y., Wang, J., Han, T., Wang, Y., He, D., Quan, W., and Ma, Z.: Using multiple linear regression method to evaluate the impact of meteorological conditions and control measures on air quality in Beijing during APEC 2014 (in Chinese), Environ. Sci., 40, 1024-1034, https://doi.org/10.13227/j.hjkx.201807044, 2019.

Li, W., Shao, L., Wang, W., Li, H., Wang, X., Li, Y., Li, W., Jones, T., and Zhang, D.: Air quality improvement in response to intensified control strategies in Beijing during 2013 − 2019, Sci. Total. Environ., 744, 140776, https://doi.org/10.1016/j.scitotenv.2020.140776, 2020.

Lin, W., Xu, X., Zhang, X., and Tang, J.: Contributions of pollutants from North China Plain to surface ozone at the Shangdianzi GAW station, Atmos. Chem. Phys., 8, 5889-5898, https://doi.org/10.5194/acp-8-5889-2008, 2008.

Lin, W., Xu, X., Ge, B., and Zhang, X.: Characteristics of gaseous pollutants at Gucheng, a rural site southwest of Beijing, J. Geophys. Res-atmos., 114, D14G, https://doi.org/10.1029/2008JD010339, 2009a.

Lin, W., Xu, X., Yu, D., Dai, X., Zhang, Z., Meng, Z., and Wang, Y.: Quality control for reactive gases observation at Longfengshan regional atmospheric background monitoring station (in Chinese), Meteorol. Mon., 35, 93-100, https://doi.org/10.7519/j.issn.1000-0526.2009.11.012, 2009b.

Lin, W., Xu, X., Ge, B., and Liu, X.: Gaseous pollutants in Beijing urban area during the heating period 2007−2008: variability, sources, meteorological, and chemical impacts, Atmos. Chem. Phys., 11, 6919-6959, https://doi.org/10.5194/acp-11-8157-2011, 2011a.

Lin, W., Xu, X., Sun, J., Li, Y., and Meng, Z.: Background concentrations of reactive gases and the impacts of long-range transport at the Jinsha regional atmospheric background station, Sci. China Earth Sci., 54, 1604-1613, https://doi.org/10.1007/s11430-011-4205-2, 2011b.

Lin, W., Xu, X., Ma, Z., Zhao, H., Liu, X., and Wang, Y.: Characteristics and recent trends of sulfur dioxide at urban, rural, and background sites in North China: Effectiveness of control measures, J. Environ. Sci., 24, 34-49, https://doi.org/10.1016/s1001-0742(11)60727-4, 2012.

Lin, W., Ma, Z., Pu, W., Gao, W., Ma, Q., and Yu, D.: Air Composition-Quality control for observation data-Reactive gases. Meteorological industry Standard of the People's Republic of China (QX/T 510–2019), 2019.

Liu, J., Zhang, X., Xu, X., and Xu, H.: Comparison analysis of variation characteristics of SO_2, NO_x, O_3 and $PM_{2.5}$ between rural and urban areas, Beijing (in Chinese), Environ. Sci., 29, 1059-1065, https://doi.org/10.3321/j.issn:0250-3301.2008.04.036, 2008.

Liu, R., Han, Z., and Li, J.: Analysis of meteorological characteristics during winter haze events in Beijing (in Chinese), Clim. Environ. Res., 19, 164-172, https://doi.org/10.3878/j.issn.1006-9585.2014.13224, 2014a.

Liu, X., Xu, X., Zhao, H., and Lin, W.: Characteristics of NO_x and CO emission on the three sites in Beijing and its surrounding areas (in Chinese), J. Saf. Environ., 14, 252-257, https://doi.org/10.13637/j.issn.1009-6094.2014.06.056, 2014b.

Liu, F., Zhang, Q., Van, D. A. R. J., Zheng, B., Tong, D., Yan, L., Zheng, Y., and He, K.: Recent reduction in NO_x emissions over China: synthesis of satellite observations and emission inventories, Environ. Res. Lett., 11, 3945-3950, https://doi.org/10.1088/1748-9326/11/11/114002, 2016.

Luo, X., Pan, Y., Goulding, K., Zhang, L., Liu, X., and Zhang, F.: Spatial and seasonal variations of atmospheric sulfur concentrations and dry deposition at 16 rural and suburban sites in China, Atmos. Environ., 146, 79-89, https://doi.org/10.1016/j.atmosenv.2016.07.038, 2016.

Meng, Z., Xu, X., Yan, P., Ding, G., Tang, J., Lin, W., Xu, X., and Wang, S.: Characteristics of trace gaseous pollutants at a regional background station in Northern China, Atmos. Chem. Phys., 9, 927-936, https://doi.org/10.5194/acp-9-927-2009, 2009a.

Meng, X., Wang, P., Wang, G., Yu, H., and Zong, X.: Variation and transportation characteristics of SO_2 in winter over Beijing and its surrounding areas (in Chinese), Clim. Environ. Res., 14, 83-91, https://doi.org/10.3878/j.issn.1006-9585.2009.03.08, 2009b.

Qi, H., Lin, W., Xu, X., and Yu, X.: Significant downward trend of SO_2 observed from 2005 to 2010 at a background station in the Yangtze Delta region, China, Sci. China. Chem., 55, 1451-7291, https://doi.org/10.1007/s11426-012-4524-y, 2012.

Qiu, X., Duan, L., Cai, S., Yu, Q., Wang, S., Chai, F., Gao, J., Li, Y., and Xu, Z.: Effect of current emission abatement strategies on air quality improvement in China: A case study of Baotou, a typical industrial city in Inner Mongolia, J. Environ. Sci.-China., 57, 383-390, https://doi.org/10.1016/j.jes.2016.12.014, 2017.

Shao, M., Tang, X., Zhang, Y., and Li, W.: City clusters in China: air and surface water pollution, Front. Ecol. Environ., 4, 353-361, https://doi.org/10.1890/1540-9295(2006)004[0353:CCICAA]2.0.CO, 2006.

Su, B., Liu, X., and Tao, J.: Pollution characteristics of SO_2, NO_x and CO in forest and mountain background region of East China (in Chinese), Environ. Monit. China., 29, 15-21, https://doi.org/10.3969/j.issn.1002-6002.2013.06.004, 2013.

Song, C., Li, R., Jianjun, H., Wu, L., and Mao, H.: Analysis of pollution characteristics of NO, NO_2 and O_3 at urban area of Langfang, Hebei (in Chinese), J. Environ. Sci.-China., 36, 2903-2912, https://doi.org/CNKI:SUN:ZGHJ.0.2016-10-004, 2016.

Steinbacher, M., Zellweger, C., Schwarzenbach, B., Bugmann, S., Buchmann, B., Ordóñez, C., Prevot, A. S. H., and Hueglin, C.: Nitrogen oxide measurements at rural sites in Switzerland: Bias of conventional measurement techniques, J. Geophys. Res-atmos., 112(D11), https://doi.org/10.1029/2006JD007971, 2007.

Sun, C., Luo, Y., and Li, J.: Urban traffic infrastructure investment and air pollution: Evidence from the 83 cities in China, J. Clean. Prod., 172, 488-496, https://doi.org/10.1016/j.jclepro.2017.10.194, 2018.

Shikwambana, L., Mhangara, P., and Mbatha, N.: Trend analysis and first time observations of sulphur dioxide and nitrogen dioxide in South Africa using TROPOMI/Sentinel-5 P data, Int. J. Appl. Earth Obs. Geoinf., 91, 102130, https://doi.org/10.1016/j.jag.2020.102130, 2020.

Tang, Y., Zhang, X., Xu, J., Zhao, X., Ma, Z., and Meng, W.: Multi-temporal scale variations of atmospheric pollutants concentrations in rural and urban areas of Beijing (in Chinese), Acta Sci. Circumst., 36, 2783-2793, https://doi.org/10.13671/j.hjkxxb.2016.0003, 2016.

UN Environment. A Review of 20 Years' Air Pollution Control in Beijing. United Nations Environment Programme, Nairobi, Kenya, 2019.

Wang, N., Lyu, X., Deng, X., Huang, X., Jiang, F., Ding, A.: Aggravating O_3 pollution due to NO_x emission control in eastern China, Science of the Total Environment, 677, 732-744, https://doi.org/10.1016/j.scitotenv, 2019.

Wang, S., Streets, D. G., Zhang, Q., He, K., Chen, D., Kang, S., Lu, Z., and Wang, Y.: Satellite detection and model verification of NO_x emissions from power plants in Northern China, Environ. Res. Lett., 5, 44007, https://doi.org/10.1088/1748-9326/5/4/044007, 2010.

Wang, S., and Hao, J.: Air quality management in China: Issues, challenges, and options, J. Environ. Sci., 24, 2-13, https://doi.org/10.1016/S1001-0742(11)60724-9, 2012.

Wang, Y., Wang, S., Song, F., Yang, J., Zhu, J., and Zhang, F.: Study on the forecast model of electricity substitution potential in Beijing – Tianjin – Hebei region considering the impact of electricity substitution policies, Energ. Policy., 144, 111686, https://doi.org/10.1016/j.enpol.2020.111686, 2020.

WMO. 2001. Global Atmosphere Watch Measurements Guide (WMO TD No. 1073). GAW Report No. #171. Geneva, Switzerland: World Meteorological Organization. Accessed on April 2, 2015. Available at ftp://ftp.wmo.int/Documents/PublicWeb/arep/gaw/gaw143.pdf.

Wu, D., Xin, J., Sun, Y., Wang, Y., and Wang, P.: Change and analysis of background concentration of air pollutants in North China during 2008 Olympic Games (in Chinese), Environ. Sci., 31, 1130-1138, https://doi.org/CNKI:SUN:HJKZ.0.2010-05-003, 2010.

Xu, X., Lin, W., Yan, P., Zhang, Z., and Yu, X.: Long-term changes of acidic gases in China's Yangtze Delta and Northeast Plain regions during 1994 – 2006 (in Chinese), Adv. Clim. Chang. Res., 4, 195-201, https://doi.org/10.3969/j.issn.1673-1719.2008.04.001, 2008.

Xu, X., Liu, X., and Lin, W.: Impacts of air parcel transport on the concentrations of trace gases at regional background stations (in Chinese), J. Appl. Meteorol. Sci., 20, 656-664, https://doi.org/10.11898/1001-7313.20090602, 2009.

Xu, W., Zhao, C., Ran, L., Lin, W., Yan, P., and Xu, X.: SO_2 noontime-peak phenomenon in the North China Plain, Atmos. Chem. Phys., 14, 7757-7768, https://doi.org/10.5194/acp-14-7757-2014, 2014.

Yang, S., Zhao, X., and Liu, N.: Impacting factors of a heavy air pollution process in autumn over Beijing (in Chinese), J. Meteorol. Environ, 13-16, https://doi.org/10.3969/j.issn.1673-503X.2010.05.003, 2010.

Yang, F., Tan, J., Zhao, Q., Du, Z., He, H., Ma, Y., Duan, F., Chen, G., and Zhao, Q.: Characteristics of $PM_{2.5}$ speciation in representative megacities and across China, Atmos. Chem. Phys., 11, 1025-1051, https://doi.org/10.5194/acp-11-5207-2011, 2011.

Yin, Q., Ma, Q., Lin, W.*, Xu, X., and Yao, J.: Measurement report: Long-term variations in surface NO_x and SO_2 from 2006 to 2016 at a background site in the Yangtze River Delta region, China, Atmos. Chem. Phys., 22, 1015–1033, https://doi.org/10.5194/acp-22-1015-2022, 2022.

Zhang, X., Zhang, P., Zhang, Y., Li, X., and Qiu, H.: The trend, seasonal cycle, and sources of tropospheric NO_2 over China during 1997−2006 based on satellite measurement, Sci China Earth Sci., 50, 8, https://doi.org/10.1007/s11430-007-0141-6, 2007.

Zhang, Q., Zheng, Y., Tong, D., Shao, M., Wang, S., Zhang, Y., Xu, X., Wang, J., He, H., Liu, W., Ding, Y., Lei, Y., Li, J., Wang, Z., Zhang, X., Wang, Y., Cheng, J., Liu, Y., Shi, Q., Yan, L., Geng, G., Hong, C., Li, M., Liu, F., Zheng, B., Cao, J., Ding, A., Gao, J., Fu, Q., Huo, J., Liu, B., Liu, Z., Yang, F., He, K., and Hao, J.: Drivers of improved $PM_{2.5}$ air quality in China from 2013 to 2017, P. Natl. Acad. Sci. Usa., 116, 24463-24469, https://doi.org/10.1073/pnas.1907956116, 2019.

Zhang, M., Shan, C., Wang, W., Pang, J., and Guo, S.: Do driving restrictions improve air quality: Take Beijing−Tianjin for example? Sci. Total Environ., 712, 136408, https://doi.org/10.1016/j.scitotenv.2019.136408, 2020.

Zhao, Y., Wang, S., Duan, L., Lei, Y., Cao, P., and Hao, J.: Primary air pollutant emissions of coal-fired power plants in China: Current status and future prediction, Atmos. Environ., 42, 8442-8452, https://doi.org/10.1016/j.atmosenv.2008.08.021, 2008.

Zhao, P. S., Dong, F., D, H., Zhao, X. J., Zhang, X. L., Zhang, W. Z., Yao, Q., and Liu, H. Y.: Characteristics of concentrations and chemical compositions for $PM_{2.5}$ in the region of Beijing, Tianjin, and Hebei, China, Atmos. Chem. Phys., 9, 4631-4644, https://doi.org/10.5194/acp-13-4631-2013, 2013.

Zhao, S., Hu, B., Gao, W., Li, L., Huang, W., Wang, L., Yang, Y., Liu, J., Li, J., Ji, D., Zhang, R., Zhang, Y., and Wang, Y.: Effect of the "coal to gas" project on atmospheric NO_x during the heating period at a suburban site between Beijing and Tianjin, Atmos. Res., 241, 104977, https://doi.org/10.1016/j.atmosres.2020.104977, 2020.

Zheng, B., Tong, D., Li, M., Liu, F., Hong, C., Geng, G., Li, H., Li, X., Peng, L., Qi, J., Yan, L., Zhang, Y., Zhao, H., Zheng, Y., He, K., and Zhang, Q.: Trends in China's anthropogenic emissions since 2010 as the consequence of clean air actions, Atmos. Chem. Phys., 18, 14095-14111, https://doi.org/10.5194/acp-18-14095-2018, 2018.

Zhong, Y., Zhou, Y., Cheng, S., Wang, X., and Shao, X.: Comparison analysis of the effect of emission reduction measures for major events and heavy air pollution in the capital (in Chinese), Environ. Sci., 41, 3449-3457, https://doi.org/10.13227/j.hjkx.201910166, 2020.

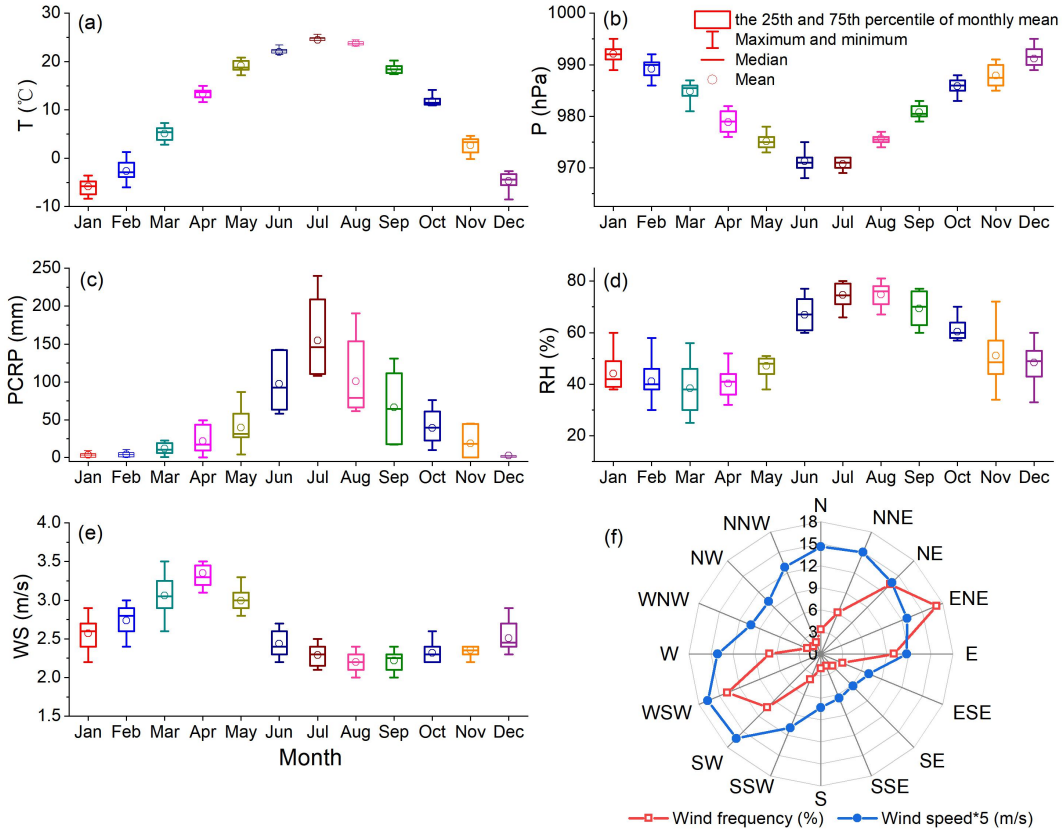

545

Figure 1. Monthly variations in **(a)** air temperature. **(b)** atmospheric pressure. **(c)** precipitation. **(d)** relative humidity. **(e)** wind speed. **(f)** wind rose map. at SDZ.

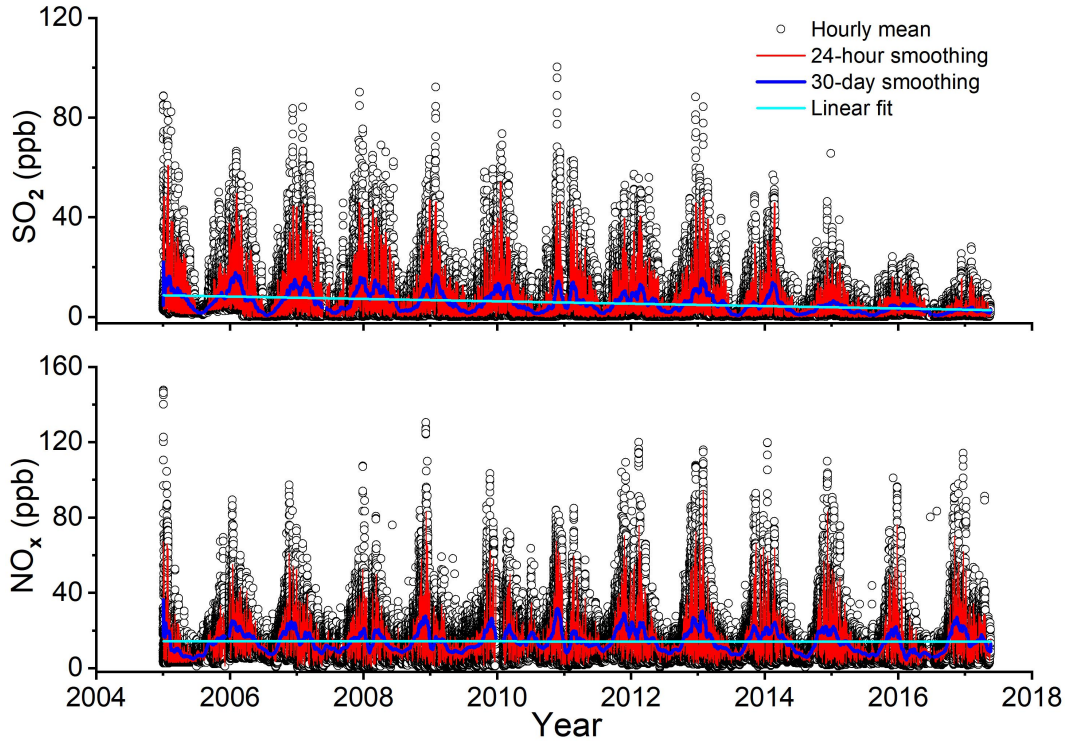

546

Figure 2. The time series variations in SO_2 and NO_x mixing ratios at SDZ.

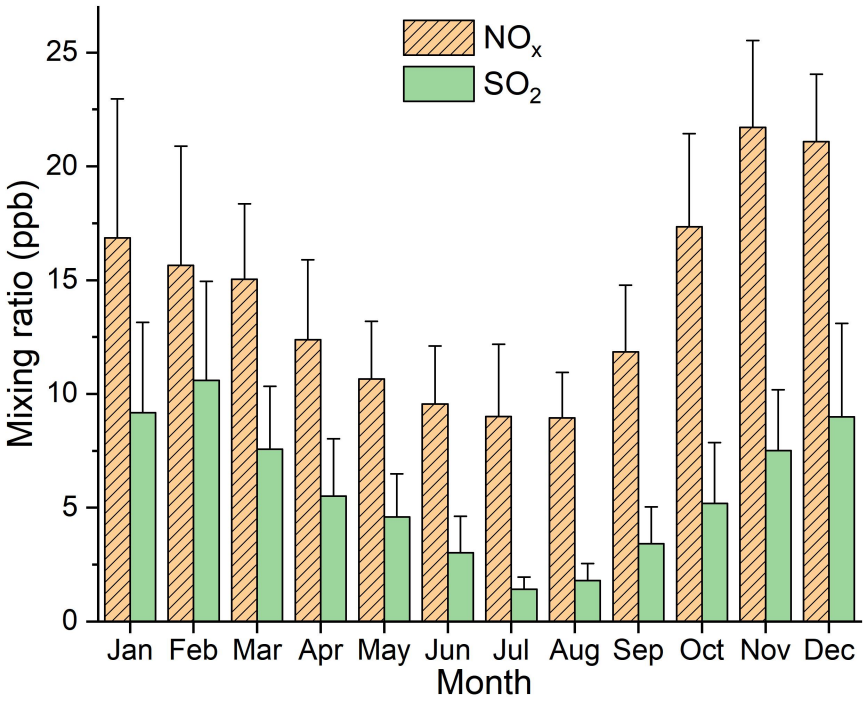

547

Figure 3. The average monthly mean of SO_2 and NO_x mixing ratios with 1 σ at SDZ.

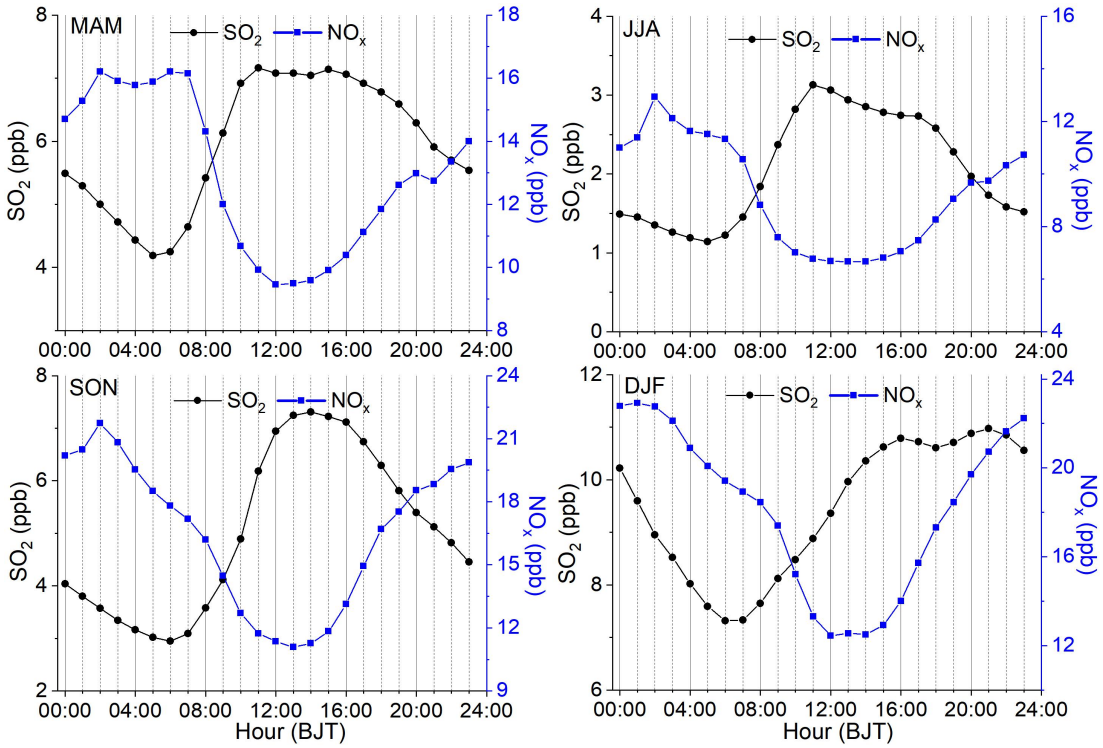

548

Figure 4. The Average diurnal variations in SO_2 and NO_x mixing ratios in four seasons at SDZ.

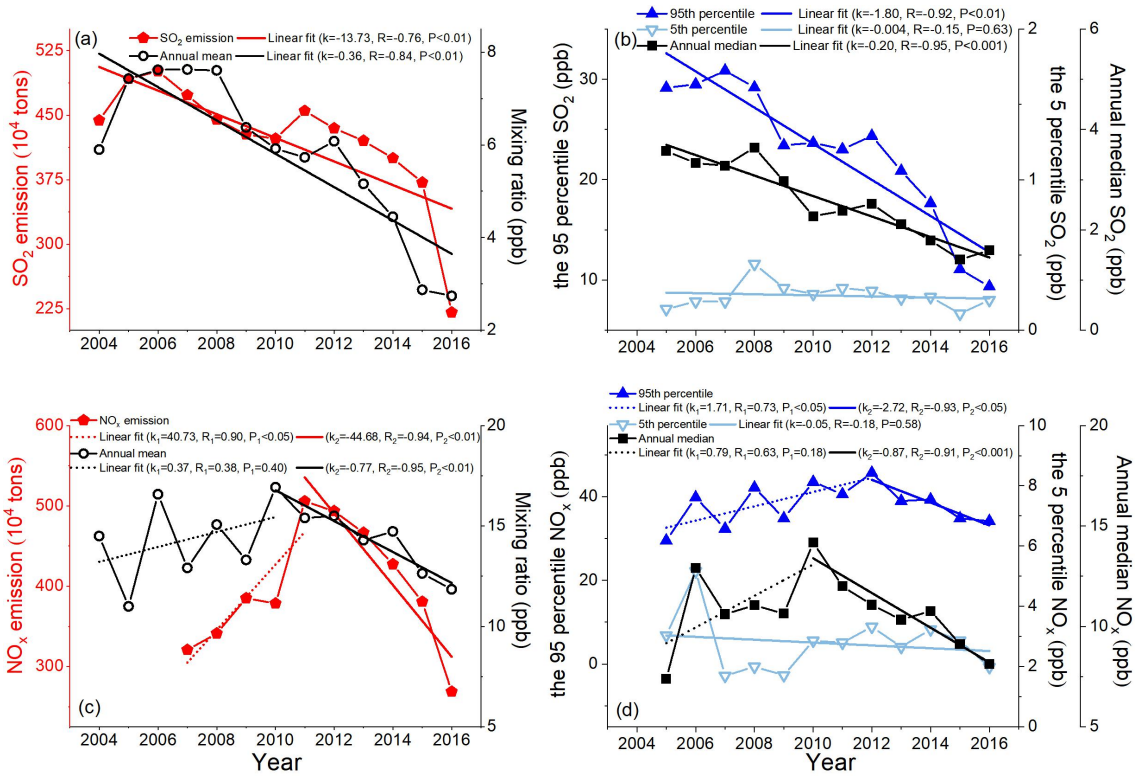

549

Figure 5. Annually variations in **(a)** SO_2 mixing ratios at SDZ and total SO_2 emissions in North China; **(b)** the 5th and 95th percentile of the hourly mean and annual median of SO_2 mixing ratios and SO_2 emissions in North China; **(c)** NO_x mixing ratios at SDZ and total NO_x emissions in North China; **(d)** the 5th and 95th percentile of the hourly mean and annual median of NO_x mixing ratios and NO_x emissions in North China. The emission data are from the 2005–2017 Yearbook of National Bureau of Statistics of China and China Statistical Yearbook on Environment provided by Ministry of Ecology and Environment of the People's Republic of China.

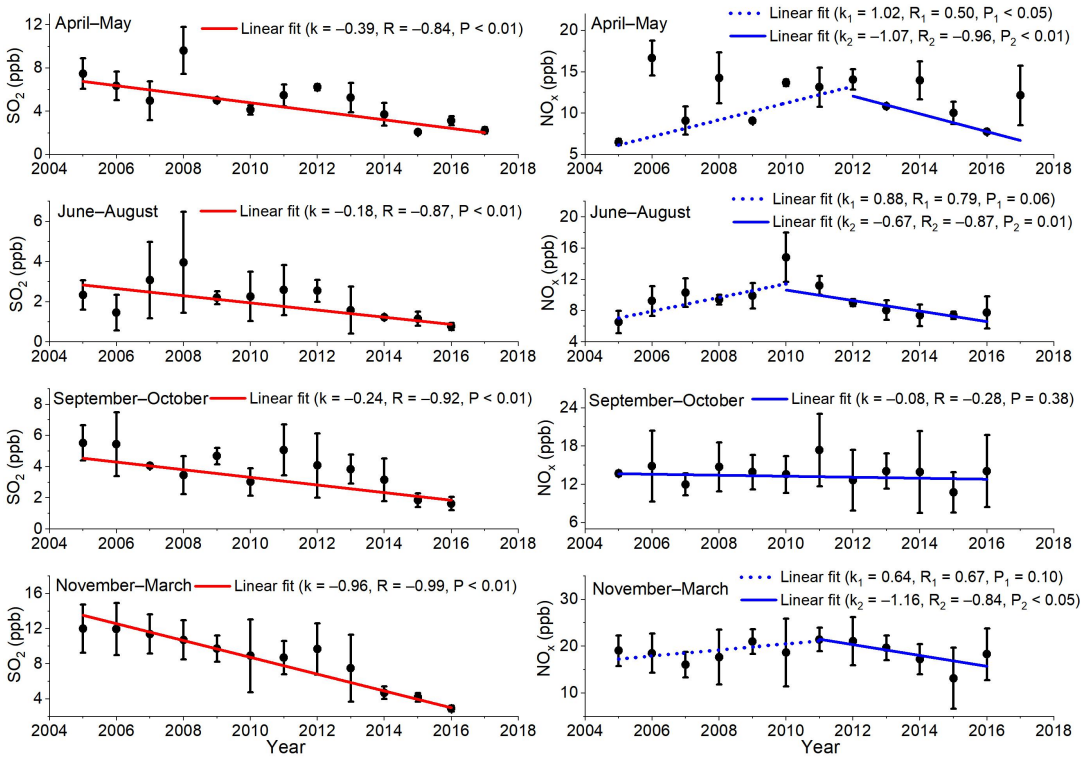

550

Figure 6. Long-term variations in monthly mean SO_2 and NO_x mixing ratios with ± 1σ in different periods at SDZ. Heating period (November–March next year), spring (April–May), summer (June–August), and autumn (September–October).

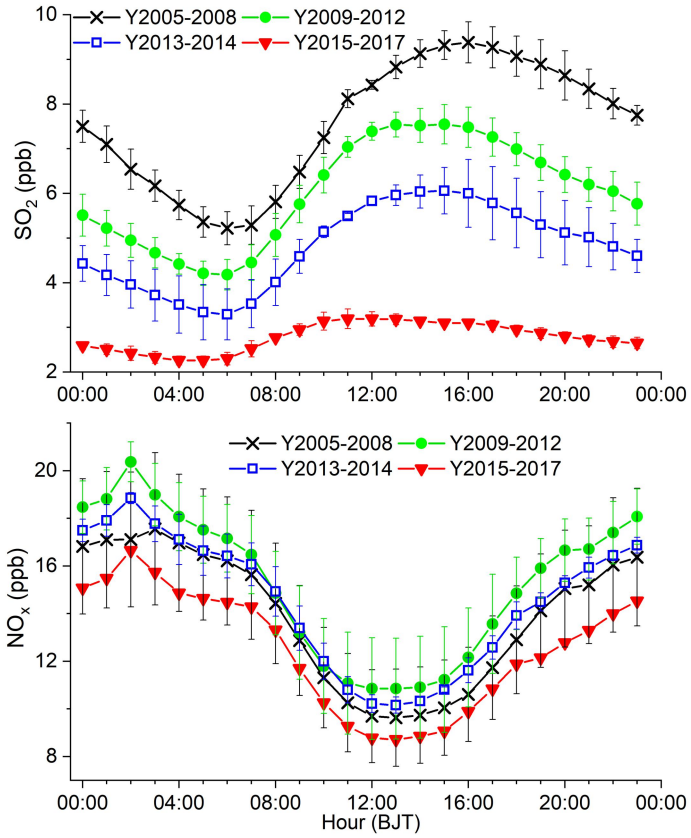

551

Figure 7. The average diurnal variations in SO_2 and NO_x mixing ratios in 4 different stages at SDZ.

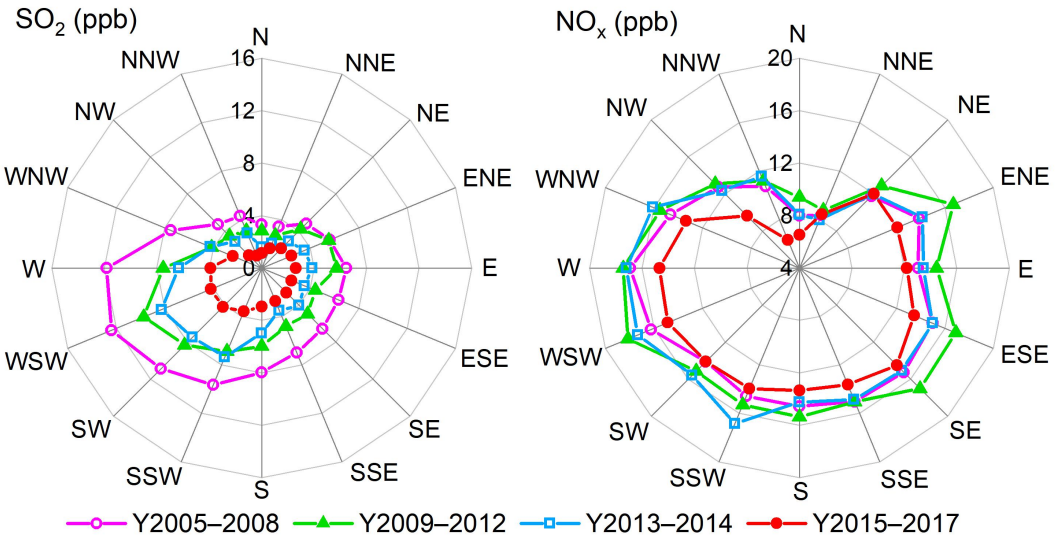

552

Figure 8. Mixing ratios of SO_2 and NO_x during different stages as a function of wind direction at SDZ.

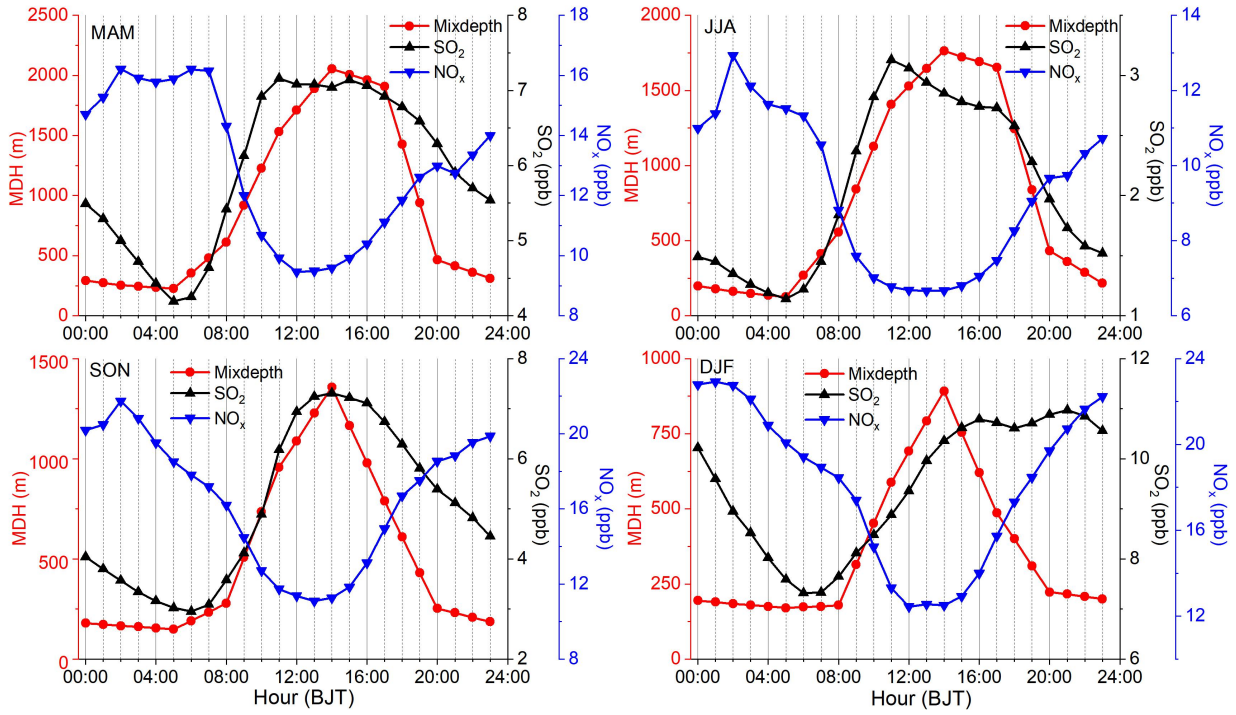

553

Figure 9. Diurnal variations in mixing depths in four seasons at SDZ.

Table 1. Statistics in the hourly mean of SO_2 and NO_x mixing ratios at SDZ.

	NO (ppb)	NO_2 (ppb)	NO_x (ppb)	SO_2 (ppb)
Mean	1.10	13.08	14.18	5.71
Standard deviation	2.58	10.89	12.36	8.44
Median	0.33	9.98	10.59	2.45
Maximum	83.34	124.41	147.58	100.34
Minimum	0.01	0.01	0.14	0.01
Count number	104923	104923	104923	105374

554

Table 2. NO_x and SO_2 levels in the atmospheric background stations in China.

Site	Time	NO_x (ppb)	SO_2 (ppb)	References
SDZ（North China）	2005.1–2017.5	14.2 ± 12.4	5.7 ± 8.4	This study
Xinglong（North China）	2005.5–2015.1	–	7.5	(Bai et al., 2015)
Linan（Yangtze River Delta）	2005.8–2006.7	–	11.1 ± 10.6	(Qi et al., 2012)
	2006.1–2016.12	13.6 ± 1.2	7.0 ± 4.2	(Yin et al., 2022)
Wuyishan（East China）	2011.3–2012.2	2.70	1.48	(Su et al., 2013)
Dinghushan（South China）	2009.1–2010.12	13.6	6.5	(Chen, 2012)
Changbaishan（Northeast China）	2009.1–2010.12	4.7	2.1	(Chen, 2012)
Fukang（Northwest China）	2009.1–2010.12	8.3	2.2	(Chen, 2012)
Gonggashan（Southwest China）	2017.1–2017.12	0.90	0.19	(Cheng et al., 2019)
Jinsha（Central China）	2006.6–2007.7	5.6 ± 5.5	2.8 ± 5.5	(Lin et al., 2011b)

555

Table 3. Trends of the hourly mean of the three sectors with the highest SO_2 level, the hourly mean of the three sectors with the lowest SO_2 level and their difference.

	Highest SO_2 values (ppb) W–WSW–SW–SSW sectors	Lowest SO_2 values (ppb) NNW–N–NNE–NE sectors	Difference (ppb)
Y2005–2008	11.18	3.96	7.23
Y2009–2012	8.12	3.20	4.91
Y2013–2014	7.36	2.35	5.01
Y2015–2017	3.95	1.48	2.48

556